

---

# Enhancement of PQ Using Adaptive Theory based Improved Linear Tracer Sinusoidal Control Strategy for DVR

---

J. Bangarraju<sup>1</sup>, V. Rajagopal<sup>2</sup>, Sabha Raj Arya<sup>3</sup> and B. Subhash<sup>4</sup>

<sup>1</sup>*B V Raju Institute of Technology, Narsapur, Medak District, Telangana, India-502313*

<sup>2</sup>*Stanley College of Engineering and Technology for Women, Abids, Hyderabad, India-500001*

<sup>3</sup>*S. V. National Institute of Technology, Surat, Gujarat, India-395007*

<sup>4</sup>*S. R. Engineering College, Warangal, Telangana, India-506371*

*E-mail: rajujbr@gmail.com, rajsarang@gmail.com, sabharaj1@gmail.com, subashbochu@gmail.com*

Received 15 April 2017; Accepted 1 August 2017;  
Publication 28 August 2017

## Abstract

This paper presents the Adaptive Theory based Improved Linear Tracer Sinusoidal (ATILS) Control Strategy for PQ Enhancement using DVR in the Distribution System. The proposed DVR effectively mitigates voltage sag/swell, unbalanced voltage sag/swell for linear loads along with harmonic compensation using ATILS Control Strategy. The DVR consists of voltage source converter (VSC), transformer with capacitor. The main advantages are more efficiency, reliability and its effective control of reactive power. The ATILS Control Strategy is used for extraction of fundamental reference load voltages quickly and accurately to mitigate PQ problems. The proposed ATILS Control Strategy for DVR is modeled using RT-LAB and MATLAB/SIMULINK and its performance is verified for various Power Quality (PQ) problems.

**Keywords:** DVR, ATILS Control Strategy, Power Quality, Harmonics, Voltage sag/swell.

*Journal of Green Engineering, Vol. 7, 189–212.*

doi: 10.13052/jge1904-4720.7129

© 2017 River Publishers. All rights reserved.

## 1 Introduction

The power quality of available supply has direct economic impact on domestic and manufacturing industries which effects the growth of the nation. This is mainly due to increasing usage of power electronics equipment in day to day life [1]. The reactive power demand and level of harmonic components are popular parameters to specify the reactive power demand at particular load and degree of distortion [2, 3]. In the low and medium power level distribution system, the most commonly occurring problems are related harmonic resonance and Power Quality (PQ). Various standards are proposed by IEEE and IEC to limit power quality problems such as IEEE 519-1992, IEEE Std. 141-1993 and IEC 1000-3-2 etc. [4–6]. The CPDs (Custom Power Devices) are used to mitigate reduction of voltage flicker, harmonic compensation, voltage sag/swell, compensation and resonance due to distortion etc. [7]. It includes DVR (Dynamic Voltage Restorer), DSTATCOM (Distribution Static Compensator) and UPQC (Unified Power Quality Conditioner) in the different configurations [8–10]. The dynamic performance of CPDs depends upon control strategy used for reference load voltage estimation and pulse generation gating scheme.

PQ problems such as voltage sag, swell, unbalance voltage sag/swell, harmonics create severe problems for present modern industry and these problems are compensated using DVR [11]. The three-leg VSC (voltage source converter), transformer with capacitor are the main components of DVR. The major advantage of proposed capacitor based DVR is that it is more efficient and reduces the cost when compared to conventional battery based DVR. Regular maintenance is required for battery based DVR and it adds additional cost for battery. The capacitor based DVR absorbs/injects active power to pre-sag/swell compensation in the distribution system [12, 13].

The design, protection and different topologies for capacitor based DVR are reported in literature [14–16]. To mitigate PQ problems the DVR has to respond quickly for extraction of reference load voltages. A few of the many control strategies for DVR are ISCT (Instantaneous Symmetrical Components Theory) [17], SRFT (Synchronous Reference Frame Theory) [18, 19], Adaline Based Control Algorithm [20], PQR Instantaneous Power Theory [21], Control Algorithm based on Space vector PWM [22], Adaptive Theory based Improved Linear Sinusoidal Control Algorithm for DSTATCOM [23] etc. SRF theory and PQ theory requires reasonable transformations and computations which takes more execution time. Adaline Algorithm requires convergence factor value is so selected to make a tradeoff between the accuracy and the rate

of convergence. ISCT Algorithm applied for DVR then it will show more oscillation the results. All these conventional control strategies take more time for extraction of reference load voltages. The DVR performance is mainly due to effective estimation of reference load voltages with proper control strategy. This paper discusses ATILS control strategy for DVR to mitigate voltage sag/swell for linear/non-linear loads, unbalanced voltage sag/swell. The proposed ATILS control strategy takes less execution time compared to conventional control strategies for generating reference load voltages [24, 25]. The ATILS based DVR is modeled using RT-LAB and MATLAB/SIMULINK and its performance results are validated at different PQ problems.

## 2 DVR Configuration and Control Algorithm

The ATILS Control Strategy based DVR for generating reference load voltages is shown in Figure 1 along with distribution system. In this proposed control strategy, the phase source voltages ( $v_{sa}, v_{sb}, v_{sc}$ ), load voltages ( $v_{La}, v_{Lb}, v_{Lc}$ ), phase source currents ( $i_{sa}, i_{sb}, i_{sc}$ ), load currents ( $i_{La}, i_{Lb}, i_{Lc}$ ), dc bus voltage ( $v_{dc}$ ) and terminal PCC voltages ( $v_t$ ) are used for estimation of load reference voltages ( $v_{La}^*, v_{Lb}^*, v_{Lc}^*$ ) based on adaptive theory based improved linear tracer sinusoidal control strategy. In the proposed ATILS Control Strategy based DVR, source currents ( $i_{sa}, i_{sb}, i_{sc}$ ) are equal to load currents ( $i_{La}, i_{Lb}, i_{Lc}$ ). To mitigate ripple currents, three inductors ( $L_f$ ) are used at the VSC and a three phase resistor ( $R_f$ ) & capacitor ( $C_f$ ) are connected at the DVR injecting transformer to mitigate voltage harmonics.

### 2.1 Generation of In-phase and Quadrature Unit Templates

The three-phase instantaneous source currents ( $i_{sa}, i_{sb}, i_{sc}$ ) may consist of negative sequence components and harmonics. These three phase source currents are given to band pass filters to filter harmonics and noise. The three phase source currents are represented as.

$$i_{sa} = i_{mp} \sin(\omega t) \quad (1)$$

$$i_{sb} = i_{mp} \sin(\omega t - 2\pi/3) \quad (2)$$

$$i_{sc} = i_{mp} \sin(\omega t - 4\pi/3) \quad (3)$$

The individual magnitude of each of the three phase source currents ( $i_{sa}, i_{sb}, i_{sc}$ ) are determined by squaring source currents and estimated currents ( $i_{ta}^1, i_{tb}^1, i_{tc}^1$ ) are

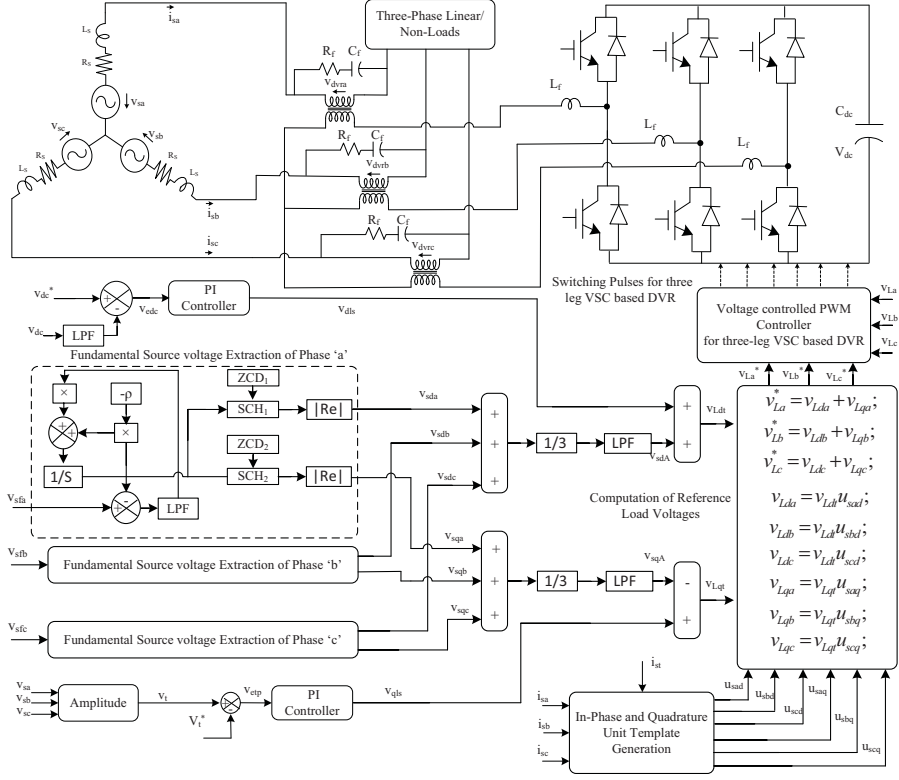


**Figure 1** ATILS Control Strategy for three-leg VSC Based DVR in the Distribution System.

$$i_{ta}^1 = [2(i_{sa}^2)]; \quad i_{tb}^1 = [2(i_{sb}^2)]; \quad i_{tc}^1 = [2(i_{sc}^2)]; \quad (4)$$

The total resultant amplitude ( $i_{st}$ ) of source currents is estimated from source current ( $i_{ta}^1, i_{tb}^1, i_{tc}^1$ ) and is given as

$$i_{st} = \sqrt{\frac{(i_{ta}^1 + i_{tb}^1 + i_{tc}^1)}{3}} \quad (5)$$

In-phase unit-templates ( $u_{sap}, u_{sbp}, u_{scp}$ ) of three phase source currents are represented as

$$u_{sap} = i_{sa}/i_{st}; \quad u_{sbp} = i_{sb}/i_{st}; \quad u_{scp} = i_{sc}/i_{st}; \quad (6)$$

The quadrature unit-templates ( $u_{saq}, u_{sbq}, u_{scq}$ ) of three phase source currents are represented as

$$u_{saq} = (-u_{sbp} + u_{scp}) / \sqrt{3} \quad (7)$$

$$u_{sbq} = (3u_{sap} + u_{sbp} - u_{sbp}) / 2\sqrt{3} \quad (8)$$

$$u_{scq} = (-3u_{sap} + u_{sbp} - u_{sbp}) / 2\sqrt{3} \quad (9)$$

## 2.2 Generation of Fundamental Active and Reactive Power Components of Load Voltages

The proposed adaptive theory based improved linear tracer sinusoidal control strategy is used to estimate fundamental active and reactive power components of load voltages of each phase as shown in the Figure 1. In the fundamental source voltage, phase 'a' component is the difference from the source voltage to estimate the error voltage signal. The filter output of the voltage signal is the combination of output voltage signal with band pass filter ( $\psi$ ) and this is multiplied with power frequency signal ( $-\rho$ ). The output of this signal is integrated to estimate phase 'a' fundamental source voltage ( $V_{sfa}$ ). Similarly other two phases 'b' and 'c' fundamental source voltages ( $V_{sfb}$  and  $V_{sfc}$ ) are estimated.

The magnitude of three phase fundamental source voltage active components ( $v_{sda}$ ,  $v_{sdb}$ ,  $v_{sdc}$ ) are extracted at positive zero crossing of in-phase unit templates. The output of ZCD<sub>1</sub> (Zero Crossing Detector) works as trigger pulse for SHC<sub>1</sub> (Sample and Hold Circuit) and fundamental voltage as a input signal of SHC<sub>1</sub>. The magnitude of fundamental active component is considered as output of SHC<sub>1</sub> real component. The average magnitude of fundamental source voltage corresponding to active power component ( $V_{sdA}$ ) is the sum of three phase fundamental source voltage active power components ( $v_{sda}, v_{sdb}, v_{sdc}$ ) divided by 3.

$$v_{sdA} = \frac{v_{sda} + v_{sdb} + v_{sdc}}{3} \quad (10)$$

Similarly, the magnitude of three phase fundamental source voltage reactive power components ( $v_{sqa}$ ,  $v_{sqb}$ ,  $v_{sqc}$ ) are extracted at positive zero crossing of quadrature-phase unit templates. The output of ZCD<sub>2</sub> (Zero Crossing Detector) works as trigger pulse for SHC<sub>2</sub> (Sample and Hold Circuit) and fundamental voltage as an input signal of SHC<sub>2</sub>. The magnitude of fundamental reactive component is considered as output of SHC<sub>2</sub> reactive component. The average magnitude of fundamental source voltage corresponding to reactive power component ( $V_{sqA}$ ) is the sum of three phase

fundamental source voltage reactive power components ( $v_{sqa}$ ,  $v_{sqb}$ ,  $v_{sqc}$ ) divided by 3.

$$v_{sqA} = \frac{v_{sqa} + v_{sqb} + v_{sqc}}{3} \quad (11)$$

### 2.3 Stability Analysis of ATILS Control Strategy

The stability analysis of ATILS Control Strategy is shown in Figure 1. The transfer function gain of low pass filter ( $G(s)$ ) is as

$$G(s) = 1 / (1 + s\tau) \quad (12)$$

Where  $\tau$  is the LPF time constant and considered as greater than zero.

The transfer function of phase 'a' is the extracted fundamental source voltage ( $v_{sfa}$ ) and source voltage ( $v_{sa}$ ) can be represented as

$$C(s) = \frac{G(s)}{H(s)} = \frac{v_{sfa}}{v_{sa}} \quad (13)$$

Where forward gain is  $G(s) = \Psi / (\tau s^2 + (\tau\rho + 1)s + (\psi + \rho))$  and feed-back gain of transfer function is  $H(s) = 1$ .

The transfer function characteristic equation can be represented as

$$\tau s^2 + (\tau\rho + 1)s + (\Psi + \rho) = 0 \quad (14)$$

Where  $\psi$  is the band pass filter frequency,  $\rho$  is the power frequency and  $\tau$  is the LPF time constant. Routh–Hurwitz criterion is used to analyze the stability of the Equation (14).

Routh–Hurwitz criterion array formation is shown in Table 1.

For the stability analysis of ATILS Control Strategy assume band pass filter frequency ( $\psi$ ) = 250 rad/sec, power frequency ( $\rho$ ) = 314.14 rad/sec and time constant ( $\tau$ ) = 0.1 sec. By substituting these values in Table 1, it was observed that there is no sign of changes in the first column of Routh–Hurwitz criterion and the characteristic roots are not positive real number. This concludes that ATILS control strategy is stable at different variations in the parameters.

**Table 1** Routh–Hurwitz criterion Table

$S^2$	$\tau$	$\Psi + \rho$
$S^1$	$\tau\rho + 1$	0
$S^0$	$\Psi + \rho$	–

## 2.4 Magnitude of Active Power Voltage Components of Reference Load Voltages

The sensed DC bus voltage ( $V_{dc} = (2\sqrt{2} V_{LL})/(\sqrt{3} m)$ ) and reference DC bus voltage ( $v_{dc}^*$ ) of VSC (Voltage Source Converter) are compared and dc bus voltage error at  $m^{\text{th}}$  sample instant is estimated as,

$$v_{edc(m)} = -v_{dc(m)} + v_{dc}^*(m) \quad (15)$$

The output error of dc bus ( $v_{edc}$ ) is feeding to PI (Proportional Integral) controller and this output is required to regulate dc bus voltage of DVR at  $m^{\text{th}}$  sample instant given as

$$v_{dls(m)} = v_{dls(m-1)} + K_{p1}(v_{edc(m)} - v_{edc(m-1)}) + K_{i1}v_{edc(m)} \quad (16)$$

Where  $v_{edc}(m)$  and  $v_{edc}(m-1)$  are the error in the DC bus voltage at  $m^{\text{th}}$  and  $(m-1)^{\text{th}}$  sample instants and  $K_{p1}$  and  $K_{i1}$  are proportional and integral gain constants.

The magnitude of active power component reference load voltage ( $V_{Ldt}$ ) is the sum of average magnitude of source voltage component ( $V_{sdA}$ ) and the DC bus PI controller output ( $v_{dls}$ ).

$$v_{Ldt} = v_{sdA} + v_{dls} \quad (17)$$

## 2.5 Magnitude of Active Power Voltage Components of Reference Load Voltages

The sensed load voltage ( $v_t$ ) and reference load voltage ( $v_t^*$ ) are compared and error at  $m^{\text{th}}$  sample instant is estimated as

$$v_{etp(m)} = -v_t(m) + v_t^*(m) \quad (18)$$

The output of error ( $v_{etp}$ ) is feeding to PI (Proportional Integral) controller and this output ( $v_{qls}$ ) is required to regulate terminal load voltage of DVR at  $m^{\text{th}}$  sample instant given as

$$v_{qls(m)} = v_{qls(m-1)} + K_{p2}(v_{etp(m)} - v_{etp(m-1)}) + K_{i2}v_{etp(m)} \quad (19)$$

Where  $v_{etp}(m)$  and  $v_{etp}(m-1)$  are the error in the load voltage PI at  $m^{\text{th}}$  and  $(m-1)^{\text{th}}$  sample instants and  $K_{p2}$  and  $K_{i2}$  are proportional and integral gain constants.

The magnitude of the reactive power component of load voltage ( $V_{Lqt}$ ) is the sum of average magnitude of source voltage component ( $V_{sqA}$ ) and the DC bus PI controller output ( $v_{qls}$ )

$$v_{Lqt} = -v_{sdA} + v_{qls} \quad (20)$$

## 2.6 Estimation of Reference Load Voltages and Switching Pulses Generation

The reference load active and reactive components of three phase voltages are estimated by using magnitude of active and reactive component of three phase load voltages using in-phase unit and quadrature unit templates

$$v_{Lda} = v_{Ldt}u_{sad}; \quad v_{Ldb} = v_{Ldt}u_{sbd}; \quad v_{Ldc} = v_{Ldt}u_{scd} \quad (21)$$

$$v_{Lqa} = v_{Lqt}u_{saq}; \quad v_{Lqb} = v_{Lqt}u_{sbq}; \quad v_{Lqc} = v_{Lqt}u_{scq} \quad (22)$$

The reference load voltages ( $v_{La}^*$ ,  $v_{Lb}^*$ ,  $v_{Lc}^*$ ) are estimated using the sum of reference active and reactive power voltage components as

$$v_{La}^* = v_{Lda} + v_{Lqa}; \quad v_{Lb}^* = v_{Ldb} + v_{Lqb}; \quad v_{Lc}^* = v_{Ldc} + v_{Lqc}; \quad (23)$$

These three phase reference load voltages ( $v_{La}^*$ ,  $v_{Lb}^*$ ,  $v_{Lc}^*$ ) are compared with actual load voltages ( $v_{La}$ ,  $v_{Lb}$ ,  $v_{Lc}$ ) and error of the output is compared with triangular carrier wave with 10 kHz frequency for generation of switching pulses DVR.

## 3 Simulation Results and Discussion

MATLAB/SIMULINK and SPS (Sim power Sytems) toolbox is used for the development of Simulink model of DVR and proposed control strategy. The performance analysis of ATILS control strategy in the time domain and DVR is simulated for voltage sag/swell for linear/non-linear loads and unbalanced voltage sag/swell using simulink model. The performance of ATILS control strategy based DVR is observed for various time varying linear/non-linear loads.

### 3.1 Performance of DVR based on ATILS Control Strategy in the Voltage Sag Operation During Linear/Non-Linear Loads

The performance of three-leg VSC based DVR on ATILS control strategy during voltage sag at linear/non-linear load is depicted in Figure 2

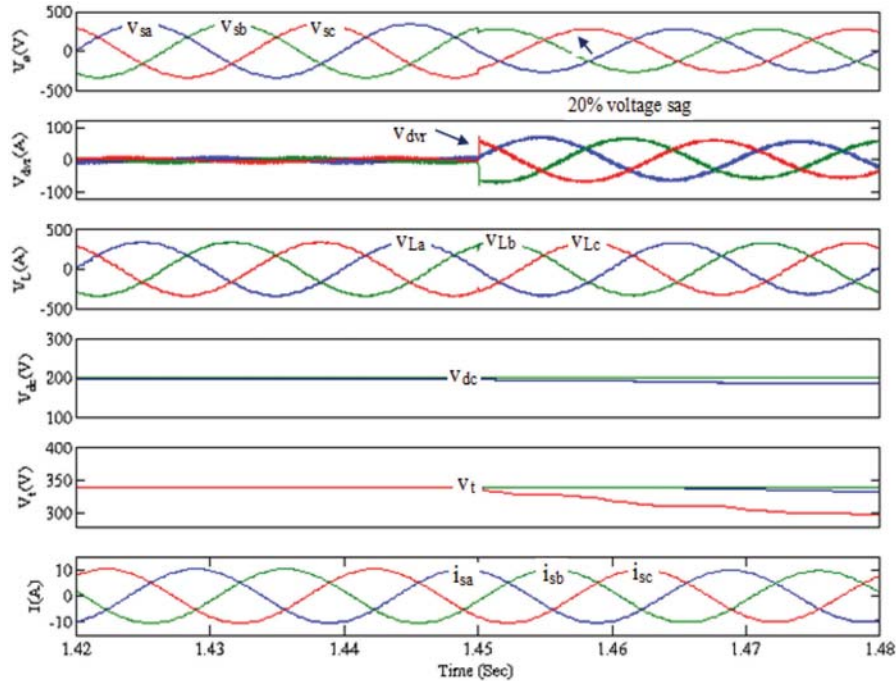


**Figure 2** Performance of ATILS Control Strategy based DVR for 20% voltage sag.

and Figure 3. The parameters of performance indices such as supply voltage ( $v_s$ ), compensating voltage ( $v_{dvr}$ ), load voltage ( $v_L$ ), dc bus voltage ( $v_{dc}$ ), terminal voltage ( $v_t$ ), load current ( $i_L$ ) at ( $t = 1.42$  sec to  $1.48$  sec) linear/non-linear loads are depicted in Figure 2–Figure 3. At  $t = 1.42$  sec the source voltage ( $v_s$ ), load current ( $i_L$ ) and load voltage ( $v_L$ ) are balanced and sinusoidal under linear loads as observed from Figure 2 and Figure 3. A 20% of voltage sag is introduced under linear loads and non-linear load at  $t = 1.45$  sec to  $1.48$  sec. The proposed ATILS Control Strategy based DVR introduces mitigating voltage in such a manner that the load voltage ( $v_L$ ) and load current ( $i_L$ ) are sinusoidal and balanced, it was observed that from Figure 2–Figure 3. The actual dc bus voltage ( $v_{dc}$ ) and its terminal voltage ( $v_t$ ) of DVR are regulated to rated values at 200 V and 339 V as shown under linear/non-linear loads. The proposed ATILS control strategy based DVR in Figure 2–Figure 3 from  $t = 1.42$  sec to  $1.48$  sec the performance parameters shows satisfactory results at voltage sag under linear/non-linear loads as per IEC and IEEE standards.

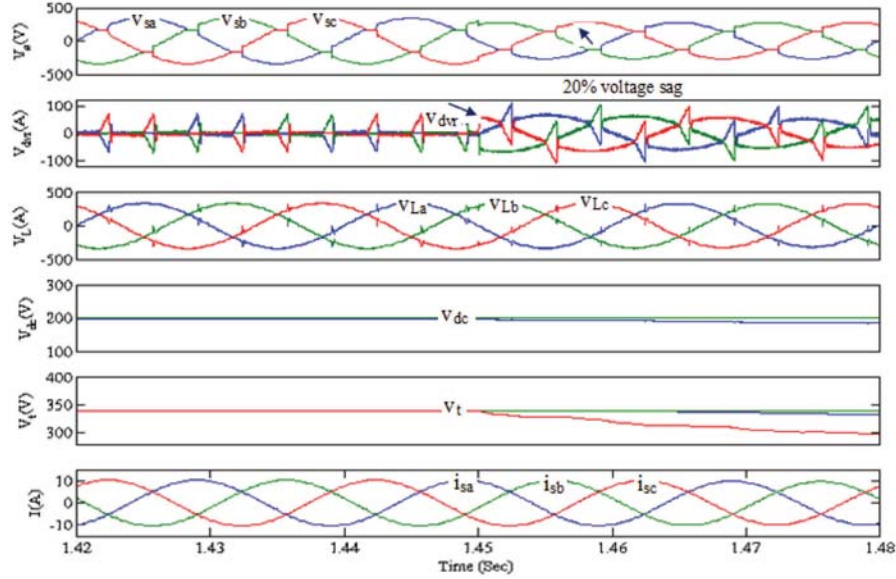


**Figure 3** Performance of ATILS Control Strategy based DVR for 20% voltage sag under non-linear loads.

### 3.2 Performance of DVR based on ATILS Control Strategy in the Voltage Swell Operation During Linear/Non-Linear Loads

The dynamic performance of three-leg VSC based DVR on ATILS control strategy during voltage swell at linear/non-linear load is depicted in Figure 4 and Figure 5. The parameters of performance indices such as supply voltage ( $v_s$ ), compensating voltage ( $v_{dvr}$ ), load voltage ( $v_L$ ), dc bus voltage ( $v_{dc}$ ), load terminal voltage ( $v_t$ ), load current ( $i_L$ ) at ( $t = 1.42$  sec to  $1.48$  sec) linear/non-linear loads are depicted in Figure 4 and Figure 5. At  $t = 1.42$  sec the source voltage ( $v_s$ ), load current ( $i_L$ ) and load voltage ( $v_L$ ) are balanced and sinusoidal under linear loads as observed from Figure 4 and Figure 5. A voltage swell of 20% is introduced under linear loads and non-linear load at  $t = 1.45$  sec to  $1.48$  sec. The proposed ATILS Control Strategy based DVR introduces mitigating voltage in such manner that the load voltage ( $v_L$ ) and load current ( $i_L$ ) are sinusoidal and balanced, it was observed that from Figure 4 to Figure 5. The proposed ATILS control strategy based DVR in Figure 4 and Figure 5 from  $t = 1.42$  sec to  $1.48$  sec the performance voltage ( $v_{dc}$ ) and terminal voltage ( $v_t$ ) of DVR are regulated to rated values at 200 V and 339 V as shown under linear/non-linear loads. During harmonic compensation of non-linear

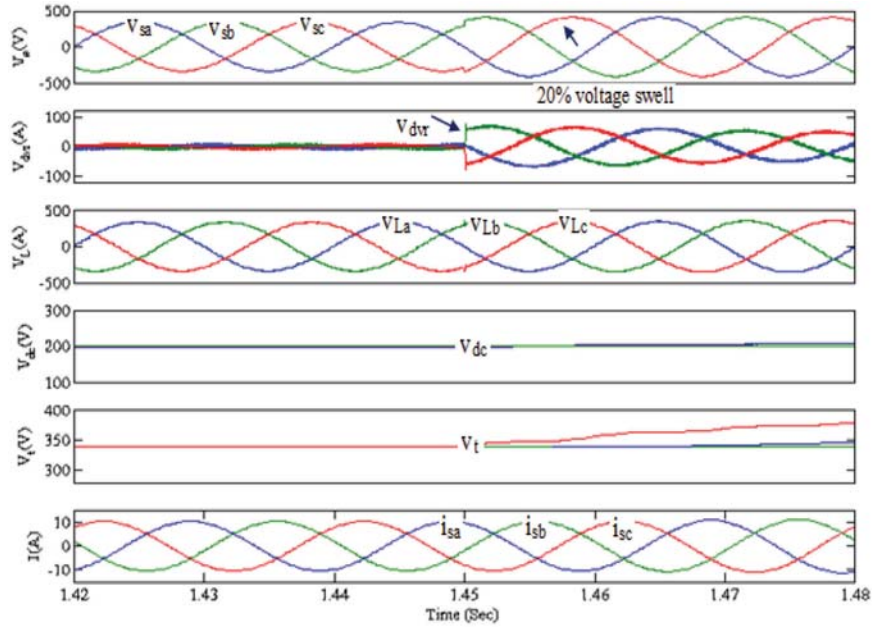


**Figure 4** Performance of ATILS Control Strategy based DVR for 20% voltage swell under linear loads.

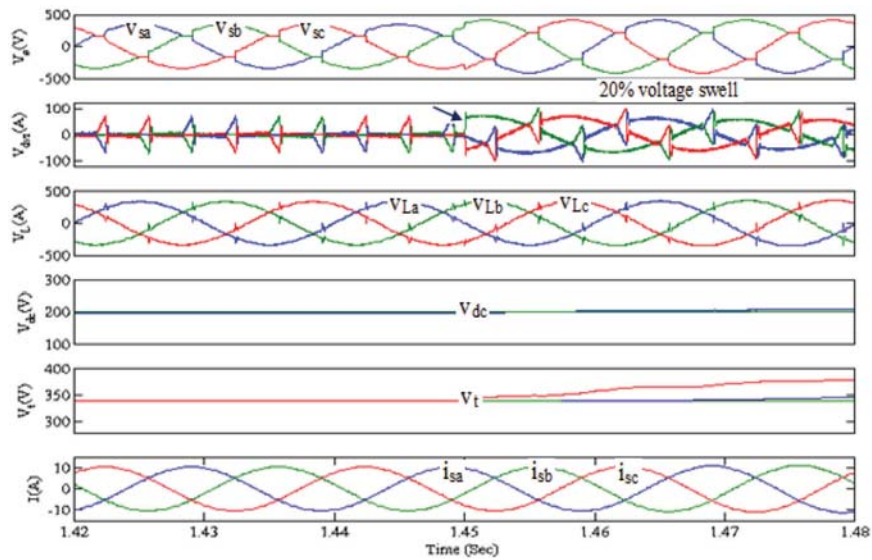


**Figure 5** Performance of ATILS Control Strategy based DVR for 20% voltage swell under non-linear loads.

load condition, THD of source voltage ( $v_s$ ) is 6.09% and THD of load voltage ( $v_L$ ) is 2.35% which are shown in Figure 8. The proposed ATILS control strategy based DVR in Figure 4 to Figure 5 from  $t = 1.42$  sec to 1.48 sec the performance parameters shows satisfactory results at voltage swell under linear/non-linear loads as per IEC and IEEE standards.

### 3.3 Performance of DVR based on ATILS Control Strategy in the Unbalanced Voltage Conditions

The dynamic performance of three-leg VSC based DVR on ATILS control strategy during voltage swell at linear/non-linear load is depicted in Figure 6 and Figure 7. The parameters of performance indices such as supply voltage ( $v_s$ ), compensating voltage ( $v_{dvr}$ ), load voltage ( $v_L$ ), dc bus voltage ( $v_{dc}$ ), terminal voltage ( $v_t$ ), load current ( $i_L$ ) at ( $t = 1.42$  sec to 1.48 sec) unbalanced linear loads are depicted in Figure 6–Figure 7. At  $t = 1.42$  sec to 1.48 sec, when one of the phase voltage is reduced to 27% of the rated nominal voltage, it was observed from Figure 6 that load voltage ( $v_L$ ) and load current ( $i_L$ ) are balanced and sinusoidal. At  $t = 1.42$  sec to 1.48 sec, when one of the phase voltage is increased to 16% of the rated voltage it was observed from

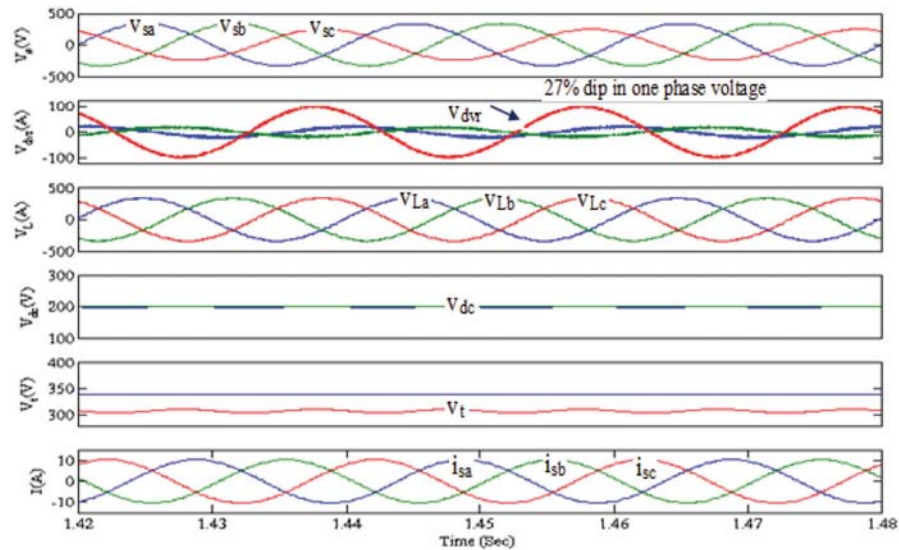


**Figure 6** Performance of ATILS Control Strategy based DVR for unbalance load at 27% less voltage in one phase.

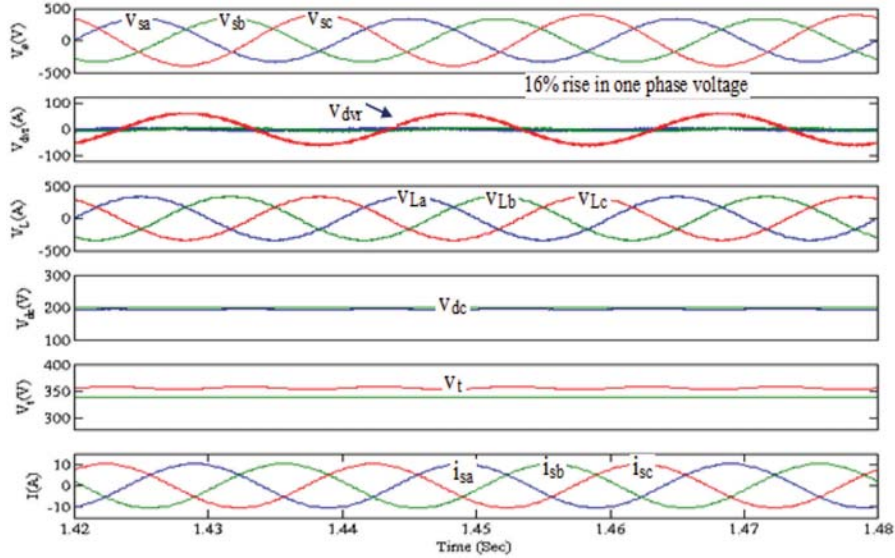


**Figure 7** Performance of ATILS Control Strategy based DVR for unbalance load at 16% more voltage in one phase.

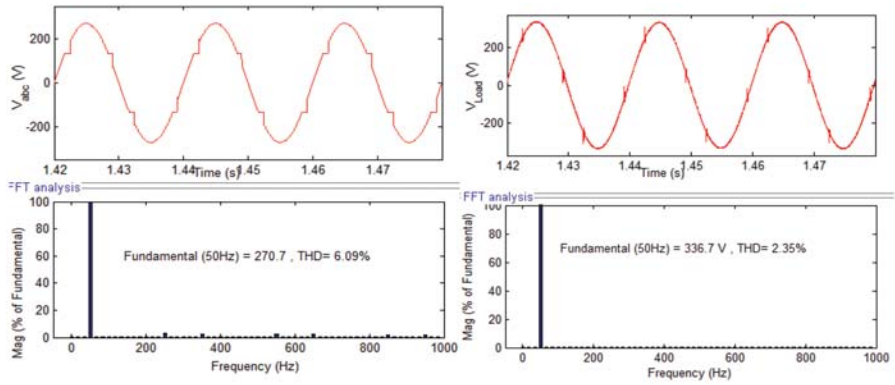


**Figure 8** Source voltage and load voltage of harmonic spectra.

Figure 7 that load voltage ( $v_L$ ) and load current ( $i_L$ ) are balanced and pure sinusoidal. The Figure 6–Figure 7 shows that DVR injecting compensating voltage such that load voltage and load current are harmonic free under voltage and over voltage at the one phase. During unbalanced load conditions DVR maintains sensed dc bus voltage and terminal voltage at 200 V and 339 V.

The proposed ATILS control strategy based DVR in Figure 6 to Figure 7 from  $t = 1.42$  sec to 1.48 sec the performance parameters shows satisfactory results at unbalanced voltage under linear/non-linear loads as per IEC and IEEE standards.

#### **4 Real Time Hardware Implementation**

A prototype 150 KVA, 415 V 50 Hz source and distribution load along with ATILS control strategy based DVR is developed and implemented using RT-LAB. A balanced linear R-L load is taken as linear load to demonstrate sag, swell, unbalanced voltages. A universal diode with R-L load is considered as consumer loads to demonstrate of harmonic Compensation. The ATILS control strategy based DVR is modeled and implemented using RT-LAB 8.2.5 with fixed step size of  $35 \mu\text{s}$  and Runge-Kutta (ODE4 solver). A three leg VSC is used as DVR for a 150 KVA, 415 V 50 Hz Y-connected system at PCC through injecting transformer and inductor filter. A dc bus capacitor value of  $3000 \mu\text{F}$  is used and is regulated at 200 V. Dynamic performance of ATILS control strategy based DVR are recorded using a Fluke 43B power analyzer.

#### **5 Hardware Results and Discussion**

The real time hardware results of ATILS control strategy based DVR under voltage sag/swell, harmonics compensation and unbalance voltages are shown in Figure 9–Figure 14. The parameters indices of distribution system such as supply voltage of ‘a’ phase ( $v_{sa}$ ), compensating voltage ( $v_{dvr}$ ), load voltage of ‘a’ phase ( $v_L$ ), dc bus voltage ( $v_{dc}$ ), source terminal voltage ( $v_{st}$ ), load terminal voltage ( $v_{Lt}$ ) are shown in Figure 9–Figure 14.

##### **5.1 Hardware Results of ATILS Control Strategy based DVR under Voltage Sag**

The hardware results of DVR on ATILS control strategy during voltage sag at linear load is depicted in Figure 9. A 20% of voltage sag is introduced under linear load condition. The proposed ATILS Control Strategy based DVR introduces mitigating voltage ( $v_{dvr}$ ) in such a manner that load voltage ( $v_{La}$ ) is balanced and sinusoidal and it maintains a voltage of 238.0 V. It was observed from Figure 9 that the dc bus voltage ( $v_{dc}$ ) is maintained at 197.9 V. The source terminal voltage ( $v_{st}$ ) and load terminal voltage ( $v_{Lt}$ ) are maintained at 312.4 V and 347.3 V in the real time hardware.

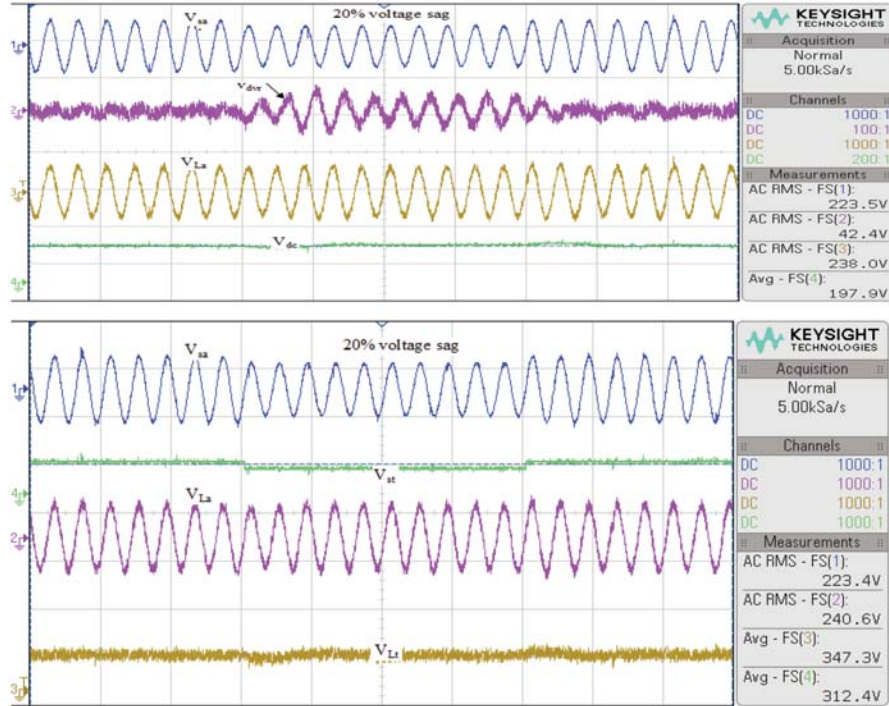


Figure 9 Hardware simulation of ATILS Control Strategy based DVR for 20% voltage sag.

### 5.2 Hardware Results of ATILS Control Strategy based DVR under Voltage Swell

The hardware results of DVR on ATILS control strategy during voltage swell at linear load is depicted in Figure 10. A voltage swell of 20% is introduced under linear load condition. The proposed ATILS Control Strategy based DVR introduces mitigating voltage ( $v_{dvr}$ ) in such a manner that the load voltage ( $v_{La}$ ) is balanced and sinusoidal and it maintains a voltage of 239.8 V. It was observed from Figure 10 that dc bus voltage ( $v_{dc}$ ) is maintained at 194.0 V. The source terminal voltage ( $v_{st}$ ) and load terminal voltage ( $v_{Lt}$ ) are maintained at 368.8 V and 352.5 V in the real time hardware.

### 5.3 Hardware Results of ATILS Control Strategy based DVR under Harmonics Compensation

The hardware results of DVR on ATILS control strategy during harmonics compensation at non-linear load is depicted in Figure 11. A highly non-linear

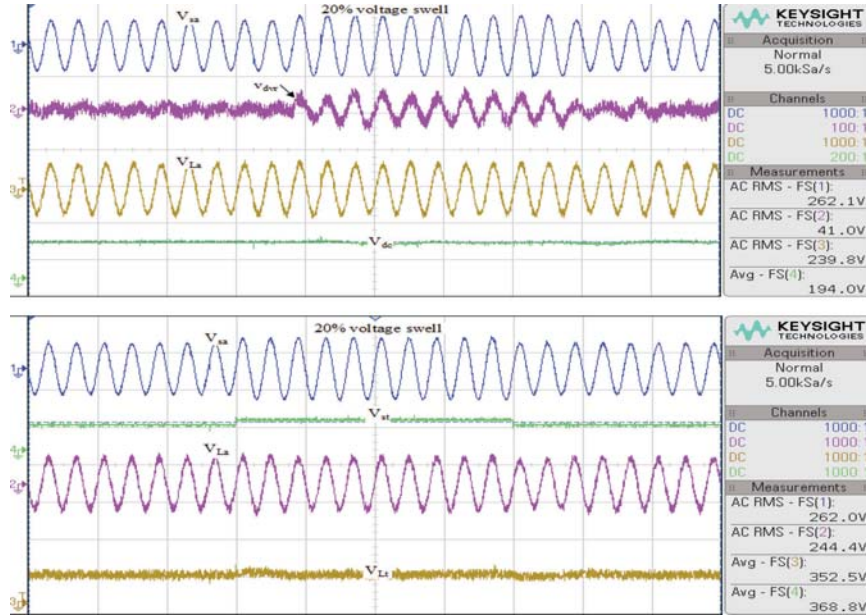


**Figure 10** Hardware simulation of ATILS Control Strategy based DVR for 20% voltage swell.

load is connected at distribution load to demonstrate harmonics compensation. The proposed ATILS Control Strategy based DVR introduces mitigating voltage ( $v_{dvr}$ ) in such a manner that load voltage ( $v_{La}$ ) is purely sinusoidal, harmonic free and it maintains a voltage of 246 V. It was observed from Figure 11 that dc bus voltage ( $v_{dc}$ ) is maintained at 191.8 V in the real time hardware. Fluke 43B power analyzer is used to demonstrate %THD of source voltage and load voltage. The source voltage of %THD of 8.9% and its fundamental voltage of 236.7 V whereas load voltage of %THD of 4.2% and its fundamental voltage of 240.0 V are shown in Figure 14.

#### 5.4 Hardware Results of ATILS Control Strategy based DVR under Unbalanced Load

The hardware results of DVR on ATILS control strategy during unbalanced at linear load is depicted in Figure 12 and Figure 13. A 27% reduced voltage in 'c' phase is introduced compared to 'a' and 'b' phases under linear load condition. The proposed ATILS Control Strategy based DVR introduces mitigating voltage ( $v_{dvr}$ ) in such a manner that load voltages ( $v_{La}$ ,  $v_{Lb}$ ,  $v_{Lc}$ )

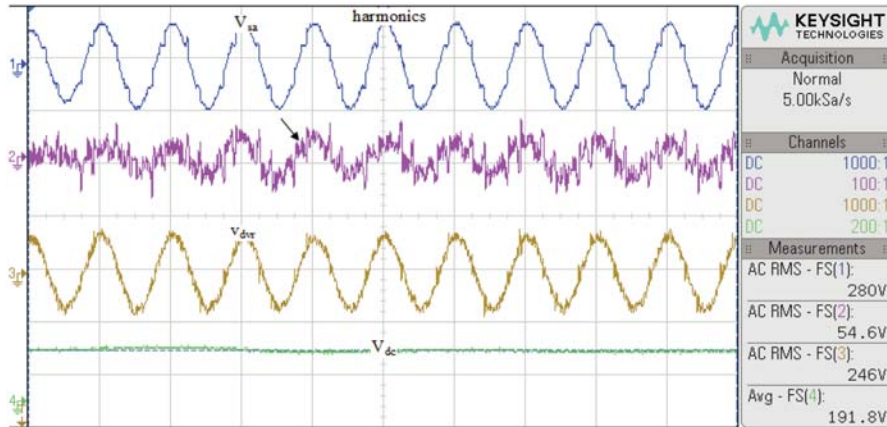


**Figure 11** Hardware simulation of ATILS Control Strategy based DVR for harmonic compensation.

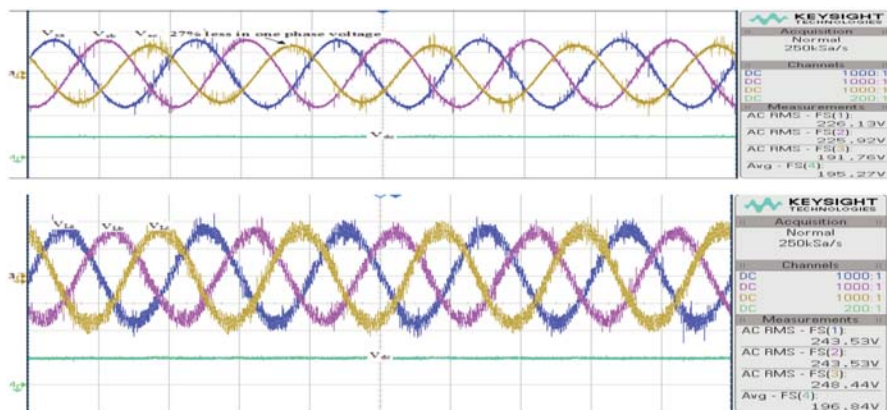


**Figure 12** Hardware simulation of ATILS Control Strategy based DVR for unbalance load at 27% less voltage in one phase.

are purely sinusoidal and highly balanced. It was observed that from Figure 12 that dc bus voltage ( $v_{dc}$ ) is maintained at 195.27 V in the real time hardware.

A 16% increased voltage in 'c' phase is introduced compared 'a' and 'b' phases under linear load condition. The proposed ATILS Control Strategy based DVR introduces mitigating voltage ( $v_{dvr}$ ) in such a manner that load voltages ( $v_{La}$ ,  $v_{Lb}$ ,  $v_{Lc}$ ) are purely sinusoidal, highly balanced. It was observed

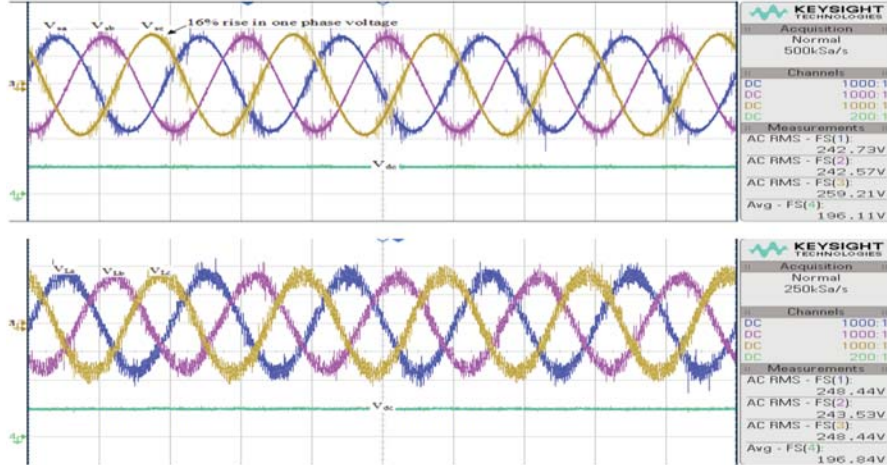


**Figure 13** Hardware simulation of ATILS Control Strategy based DVR for unbalance load at 16% rise voltage in one phase.

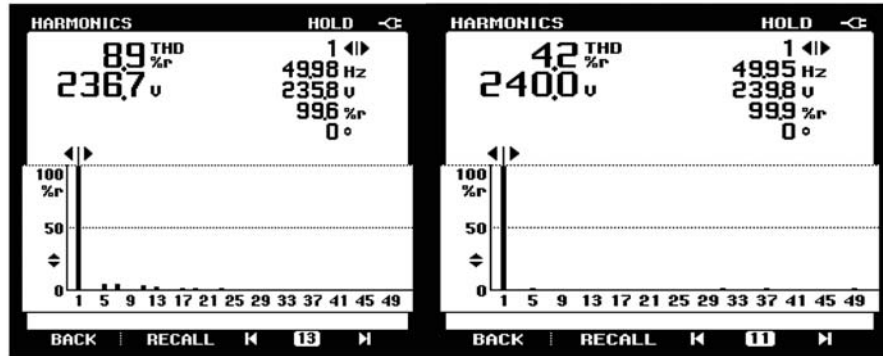


**Figure 14** Real Time harmonic spectra of source voltage ( $v_s$ ) and load voltage ( $v_L$ ).

that from Figure 14 that the dc bus voltage ( $v_{dc}$ ) is maintained at 196.11 V in the real time hardware.

## 6 Conclusion

The three leg VSC based DVR is implemented by using ATILS Control Strategy. The proposed ATILS control strategy has been used for quick and accurate extraction of reference load voltages for generation of switching

pulses of DVR. The proposed DVR is more reliable, efficient and controls reactive power. The dynamic performance of ATILS Control Strategy based DVR shows satisfactory simulation results and hardware results for PQ problems such as compensation of voltage sag/swell under linear/non-linear loads and unbalanced voltage sag/swell. Under different PQ disturbances, the sensed dc bus voltage and terminal voltage are maintained at 200 V and 339 V respectively under MATLAB simulation and hardware results. In ATILS control strategy based DVR during harmonic compensation, THD of source voltage ( $v_s$ ) is 6.09%, THD of load voltage ( $v_L$ ) is 2.35% within IEC and IEEE standards under MATLAB simulation. In ATILS control strategy based DVR during harmonic compensation, THD of source voltage ( $v_s$ ) is 8.9%, THD of load voltage ( $v_L$ ) is 4.2% within IEC and IEEE standards under hardware.

## Appendix

The ATILS Control Strategy based DVR parameters are:

Supply voltage: 415 V, 50 Hz

Source Impedance:  $R_s = 0.1 \Omega$ ,  $L_s = 1 \text{ mH}$

Consumer loads: Non-Linear Load – 3- $\Phi$  diode bridge rectifier with  $R = 4 \Omega$  and  $L = 500 \text{ mH}$ .

Linear Load –  $15 \Omega$  and  $100 \text{ mH}$

Ripple filter:  $R_f = 5.0 \Omega$  and  $C_f = 5.0 \mu\text{F}$  (for 10 kHz PWM frequency)

DC voltage PI controller:  $k_{p1} = 1.412$ ,  $k_{i1} = 1.602$

AC voltage PI controller:  $k_{p2} = 3.31$ ,  $k_{q2} = 5.14$

DC bus capacitor  $C_{dc} = 3000 \mu\text{F}$

AC inductor:  $2.99 \text{ mH}$

Transformer: 15 kVA, 100 V/400 V per transformer

## References

- [1] Ortiz, A., Gherasim, C., Manana, M., Renedo, C. J., Eguiluz, L. I., and Belmans, R. J. M. (2005). Total harmonic distortion decomposition depending on distortion origin. *IEEE Trans. Power Del.* 20, 2651–2656.
- [2] Dugan, R. C., McGranaghan, M. F., and Beaty, H. W. (2006). *Electric Power Systems Quality*, 2nd edn. New York, NY: McGraw-Hill.
- [3] Padiyar, K. R. (2008). *FACTS Controllers in Power Transmission and Distribution*. New Delhi: New Age Int.

- [4] IEEE Std (1992). *IEEE Recommended Practices and Requirement for Harmonic Control on Electric Power System*. Piscataway, NJ: IEEE Standards Association, 519.
- [5] IEEE Std (1993). *IEEE Recommended Practice for Electric Power Distribution for Industrial Plants, IEEE Std*. Piscataway, NJ: IEEE Standards Association, 141.
- [6] Electromagnetic Compatibility (EMC). (1995). *Part 3: Limits-Section 2: Limits for Harmonic Current Emissions (Equipment Input Current > 16 A per Phase) IEC1000-3-2 Document*, 1st Edn. Piscataway, NJ: IEEE Standards Association.
- [7] Lee, T. L., and Hu, S. H. (2011). Discrete frequency-tuning active filter to suppress harmonic resonances of closed-loop distribution power systems. *IEEE Trans. Power Electron.* 26, 137–148.
- [8] Wu, J.-C., Jou, H. L., Feng, Y. T., Hsu, W. P., Huang, M. S. and Hou, W. J. (2007). Novel circuit topology for three-phase active power filter. *IEEE Trans. Power Del.* 22, 444–449.
- [9] Singh, B., Jayaprakash, P., and Kothari, D. P. (2008). Power factor correction and power quality improvement in the distribution system. *Elect. India Mag.* 2008, 40–48.
- [10] Yao, Z., and Xiao, L. (2013). Control of single-phase grid-connected inverters with nonlinear loads. *IEEE Trans. Ind. Electron.* 60, 1384–1389.
- [11] Fuchs, E. F., and Mausoum, M. A. S. (2008). *Power Quality in Power Systems and Electrical Machines*. London: Elsevier.
- [12] Fuchs, E. F., and Mausoum, M. A. S. (2008). *Power Quality in Power Systems and Electrical Machines*. London: Elsevier Academic Press.
- [13] Akagi, H., Watanabe, E. H. and Aredes, M. (2007). *Instantaneous power theory and applications to power conditioning*. Hoboken NJ: John Wiley and Sons.
- [14] Dahler, P., and Knap, G. (2013). Protection of a dynamic voltage restorer. US Patent 6633092.
- [15] Ghosh, A., Jindal, A. K. and Joshi, A. (2004). Design of a capacitor supported dynamic voltage restorer (DVR) for unbalanced and distorted loads. *IEEE Trans. Power Deliv.* 19, 405–413.
- [16] Nielsen, G. J., and Blaabjerg, F. (2005). A detailed comparison of system topologies for dynamic voltage restorers. *IEEE Trans. Ind. Appl.* 41, 1272–1280.
- [17] Ghosh, A., and Joshi, A. (2002). A new algorithm for the generation of reference voltages of a DVR using the method of instantaneous symmetrical components. *Power Eng. Rev. IEEE* 22, 63–65.

- [18] Jayaprakash, P., Singh, B., Kothari, D. P., Chandra, V., AlHaddad, H. (2008). Control of reduced rating dynamic voltage restorer with battery energy storage system,” in *Proceedings of the Power System Technology and IEEE Power India Conference*, Delhi, 1–6.
- [19] Ibrahim, A. O., Nguyen, T. H., Lee, D. C., Kim, S. C. (2011). A fault ride-through technique of DF/G wind turbine systems’ using dynamic voltage restorers. *IEEE Trans. Energy Conv.* 26, 871–882.
- [20] Singh, B., Jayaprakash, P. and Kothari, D. P. (2009). Adaline based control of capacitor supported DVR for distribution systems. *J. Power Electron.* 9, 3.
- [21] Lee, S.-J., Kim, H., SuI, S.-K., and Blaabjerg, F. (2004). A novel control algorithm for static series compensators by use of PQR instantaneous power theory. *IEEE Trans. Power Electron.* 19, 814–827.
- [22] Ding, H., Shuangyan, S., Zhong, D. X., and Jun, G. (2002). Anovel dynamic voltage restorer and its unbalanced control strategy based on space vector PWM. *Int. J. Elect. Power Energy Syst.* 24, 693–699.
- [23] Singh, B., and Arya, S. R. (2013). Adaptive theory based improved linear sinusoidal tracer control algorithm for DSTATCOM. *IEEE Trans. Power Electron.* 28, 3768–3778.
- [24] Bangarraju, J., Rajagopal, V., and Jayalaxmi, A. (2014). “Implementation of three-leg VSC based DVR using IRPT control algorithm,” in *Proceedings of the 6th IEEE India International Conference on Power Electronics*, Delhi, 1–6.
- [25] Bangarraju, J., Rajagopal, V., Rosila, D., Jebarani and Madhuri, C. L. (2016). “A new  $v\cos\phi$  control scheme of capacitor supported DVR for power quality improvement”, in *Proceedings of the IEEE International Conference On Power & Energy Systems Towards Sustainable Energy*, Rome, 1–7.

## Biographies



**J. Bangarraju** was born in Tanuku, India, in 1982. He received the B.Tech. degree in Electrical and Electronics Engineering from A.S.R College of Engineering, Tanuku in 2004 and the M.Tech. degree from JNTU, Hyderabad in 2007. Presently working as Associate Professor in B V Raju Institute of Technology, Narsapur, Telangana, India. His area of interest includes power electronics and drives, power quality, FACTS and Artificial neural networks. He is currently working towards Ph.D. degree at the Department of Electrical Engineering, JNTU Hyderabad, India. He is a life member of the Indian Society for Technical Education (ISTE) and Member of the Institute of Electrical and Electronics Engineers (IEEE).



**V. Rajagopal** was born in Kazipet, Warangal, India in 1969. He received the AMIE (Electrical) degree from The Institution of Engineers (India), in 1999, M.Tech. degree from the Uttar Pradesh Technical University India in 2004 and Ph.D. degree in Indian Institute of Technology (I.I.T.) Delhi India, in 2012. Presently working as Professor and HOD in Stanley College of Engineering and Technology for Women, Hyderabad, Telangana, India. His area of interest includes power electronics and drives, renewable energy generation and applications, FACTS, and power quality. He is a life member of the Indian Society for Technical Education (ISTE), Fellow of Institution of Engineers (India) (IE (I)) and a Member of the Institute of Electrical and Electronics Engineers (IEEE).



**Sabha Raj Arya** received Bachelor of Engineering (Electrical Engineering) degree from Government Engineering College Jabalpur, in 2002, Master of Technology (Power Electronics) from Motilal National Institute of Technology, Allahabad, in 2004 and Ph.D. degree from Indian Institute of Technology (I.I.T.) Delhi, New Delhi, India, in 2014. He is joined as Assistant Professor, Department of Electrical Engineering, Sardar Vallabhbhai National Institute of Technology, Surat. His fields of interest include power quality, design of power filters and distributed power generation.

He received Two National Awards namely INAE Young Engineer Award from Indian National Academy of Engineering, POSOCO Power System Award from Power Grid Corporation of India in the year of 2014 for his research work. He has also received Amit Garg Memorial Research Award-2014 from I.I.T. Delhi from the high impact publication in a quality journal during the session 2013–2014. He is a Senior Member of the Institute of Electrical and Electronics Engineers (IEEE).



**Bochu Subhash** is a Ph.D. Student at Jawaharlal Nehru Technological University Hyderabad Kukatpally, Hyderabad since 2012. Received B.Tech. degree in Electrical and Electronics Engineering from RGM CET, Nandyal in 2001 then went on to pursue M.Tech. Course in Energy System from Visveswaraiiah Technological University, Belugum, Karnataka in 2004. He is presently working as Sr. Assistant Professor and has been delivering various administration works in reputed Autonomous Engineering College, Warangal, Telangana, India. His area of interest includes power electronics and drives, power quality, wind power generation and smart metering system.

